Surface enhanced Raman spectroscopic direct determination of low molecular weight biothiols in umbilical cord whole blood†

Julia Kuligowski,[a] Marwa R. EL-Zahry,[b,c] Ángel Sánchez-Illana,[a] Guillermo Quintás,[d,e] Máximo Vento[a,f,g] and Bernhard Lendl*[b]

Biothiols play an essential role in a number of biological processes in living organisms including detoxification and metabolism. Fetal to neonatal transition poses a pro-oxidant threat for newborn infants, especially those born prematurely. A reliable and rapid tool for the direct determination of thiols in small volume whole blood (WB) samples would be desirable for its application in clinical practice. This study shows the feasibility of Surface Enhanced Raman Spectroscopy (SERS) using a silver colloid prepared by reduction of silver nitrate using hydroxylamine, as the SERS substrate for the quantification of thiols in WB samples after a simple precipitation step for protein removal. Bands originating from biothiols (790, 714 and 642 cm^{-1}) were enhanced by the employed SERS substrate and the specificity of the detected SERS signal was tested for molecules presenting −SH functional groups. A statistically significant correlation between the obtained SERS signals and the thiol concentration measured using a chromatographic reference method in umbilical cord WB samples could be demonstrated. Using WB GSH concentrations obtained from the chromatographic reference procedure, a Partial Least Squares (PLS) regression model covering GSH concentrations from 13 to 2200 μM was calculated obtaining a root mean square error of prediction (RMSEP) of 381 μM when applied to an external test set. The developed approach uses small blood sample volumes (50 μL), which is important for clinical applications, especially in the field of neonatology. This feasibility study shows that the present approach combines all the necessary characteristics for its potential application in clinical practice.

1. Introduction

Biological thiols are essential in living organisms and are involved in a number of biological processes, such as the transsulfuration pathway, the methionine cycle and the

[a]*Neonatal Research Unit, Health Research Institute Hospital La Fe, Avda Fernando Abril Martorell 106, 46026 Valencia, Spain*

[b]*Institute of Chemical Technologies and Analytics, Vienna University of Technology, Getreidemarkt 9/151, A-1060 Vienna, Austria. E-mail: bernhard.lendl@tuwien.ac.at; Fax: +43/1 58801 15199; Tel: +43/1 58801 15140*

[c]*Department of Pharmaceutical Analytical Chemistry, Faculty of Pharmacy, Assiut University, 71526 Assiut, Egypt*

[d]*Safety & Sustainability, Leitat Technological Center, Avda Fernando Abril Martorell 106, 46026 Valencia, Spain*

[e]*Analytical Unit, Health Research Institute Hospital La Fe, Avda Fernando Abril Martorell 106, 46026 Valencia, Spain*

[f]*Division of Neonatology, University & Polytechnic Hospital La Fe, Avda Fernando Abril Martorell 106, 46026 Valencia, Spain*

[g]*National Coordinator Spanish Maternal and Child Health and Development Network SAMID, Instituto Carlos III (Spanish Ministry of Economy and Competitiveness), Spain*

†Electronic supplementary information (ESI) available. See DOI: 10.1039/c5an01865j

γ-glutamyl cycle.[1] In human blood and tissues, biothiols including reduced glutathione (γ-glutamyl–cysteinyl–glycine, GSH), cysteine, homocysteine, *N*-acetylcysteine, cysteinylglycine, γ-glutamylcysteine, cysteamine and coenzyme A are found. GSH is an important redox-active biomolecule with critical functions involved in the maintenance and regulation of cellular and organismal health.[2] GSH deficiency predisposes to oxidative damage which is thought to contribute to the onset and progression of many disease states.[3] In asphyxiated newborn infants, the glutathione/oxidized glutathione (GSH/GSSG) ratio is substantially reduced when resuscitated with 100% oxygen instead of room air (21%). Moreover, this alteration persists even four weeks after birth revealing protracted oxidative stress.[4] Very preterm infants lack the expression of γ-cystathionase and are therefore incapable of synthesizing cysteine and as a consequence, GSH. Under these circumstances preterm infants are predisposed to oxidative stress when treated with oxygen supplementation.[5]

Biothiols are prone to enzymatic and non-enzymatic oxidation after sample collection during sample storage and processing. A number of strategies have been proposed to minimize this potential source of error, including the addition

of a chelating agent (*e.g.* ethylenediaminetetraacetic acid, EDTA) as an anti-coagulant during blood extraction, sample acidification or alkylation of reduced thiol groups using *e.g.* *N*-ethylmaleimide (NEM).[6] Nonetheless, sample pretreatment in clinical practice is often troublesome. Even apparently straightforward procedures are very difficult to implement. These drawbacks justify new efforts to develop methods for a fast and direct quantification of the GSH levels in blood. The direct determination of GSH blood levels would have a tremendous impact on the robustness of the data provided and it would facilitate the comparison of data across different clinical studies.

GSH is the most abundant low-molecular-mass sulfhydryl group (–SH) containing, non-protein tripeptide thiol and comprises over 98% of all thiols in most tissues with the exception of kidneys. In the human blood, GSH concentrations for plasma ranging between 1 and 5 μM have been reported, whereas in whole blood (WB), GSH concentrations in the mM range are found, as over 95% of GSH is located inside the erythrocytes.[1,3] Due to the biological and clinical importance of GSH, the demand for robust analytical methods for its determination is increasing. A wide range of analytical methodologies has been proposed including immunoassays, colorimetric and fluorimetric assays as well as approaches employing different separation techniques coupled with spectroscopic and electrochemical detection systems.[1,7–11] Due to its high sensitivity, specificity and precision, LC separation with spectroscopic detection is frequently the method of choice. However, in the clinical setting, there is a need for automatized and faster analysis methods embedded in portable sensing systems.[1]

Optical technologies have been heavily investigated for the development of portable sensing systems and devices.[12,13] Raman spectroscopy has several major advantages for low molecular weight biothiol detection over other techniques such as UV or fluorescence spectroscopy, due to the lack of chromophors and fluorophors, or infrared spectroscopy that is suffering from low sensitivity. Raman spectroscopy provides direct molecular specific information on biothiols and shows very low background signal in the fingerprint region when analyzing aqueous samples. Moreover, the development of Surface Enhanced Raman Spectroscopy (SERS) yields increased sensitivity levels and opens the possibility of developing a wide range of Raman-based biomedical applications. For a detailed description of Raman and SERS based applications in the field of biomedicine the reader is referred to recently published review articles.[14–16] It has been shown that SERS may provide detection limits of the same order of magnitude as fluorescence spectroscopy, with the additional advantage of multiplexing capability. Hence, SERS simultaneously provides molecular specific information and high sensitivity and specificity.[14,15]

Because of that there is growing interest in the use of Raman and SERS for the detection of biothiols and GSH in biological samples. Raman spectroscopy was employed to study the changes in the intensity of S–H and S–S bonds in the lenses of guinea pigs upon treatment[17] as well as for studying oxidative stress in trapped erythrocytes.[18] SERS has been previously employed for improving the sensitivity of Raman detection of GSH by relying on the bonding of the thiol group to Au or Ag nanoparticles (NPs). On the one hand side SERS detection of GSH using reversed reporting agents has been proposed for aqueous GSH solutions[19] as well as intracellular GSH[20,21] and GSH in WB.[21] The direct determination of GSH in aqueous solutions using SERS has been proposed repeatedly[22–24] and very recently SERS using Ag NPs has been proposed for the monitoring of GSH oxidation in plasma samples under non-thermal irradiation.[25] However, to the best of our knowledge, direct measurements in WB samples have not yet been reported. The analysis of body fluids can provide a snapshot of clinically relevant information about the human health at the moment of analysis. However, the development of direct spectroscopic analysis methods is very demanding due to the extremely complex composition of samples originating from countless metabolic processes, and the differences in the metabolite concentration ranges across biofluids. Consequently, each type of body fluid and metabolite typically requires a dedicated assay.[14]

The aim of this study was to demonstrate the feasibility of a direct approach for the rapid and quantitative determination of low molecular weight biothiols in umbilical cord WB samples. SERS detection was carried out on a confocal Raman microscope employing silver NPs after a single sample processing step involving the acidic precipitation of proteins. Specificity and correlation of SERS signal and biothiol concentration could be demonstrated by comparing the results obtained from the analysis of a set of umbilical cord blood samples by SERS and a reference method employing ultra performance liquid chromatography coupled to tandem mass spectrometry (UPLC-MS/MS). The reduced sample pretreatment, analysis time and sample volume, especially critical in the field of neonatology, required by the proposed approach will facilitate the potential application of SERS-based assays for biothiol analysis in clinical practice.

2. Material and methods

2.1 Chemicals and reagents

Methanol and perchloric acid were of analytical grade. Silver nitrate, hydroxylamine hydrochloride, sodium hydroxide, NEM, glycine, reduced and oxidized glutathione (GSH and GSSG, respectively), γ-L-glutamyl–L-cysteine, L-homocysteine and L-amino acid standards including L-alanine, L-arginine hydrochloride, L-asparagine, L-aspartic acid, L-cysteine hydrochloride, L-cystine, L-glutamic acid, L-glutamine, L-histidine hydrochloride, *trans*-4-hydroxy-L-proline, L-isoleucine, L-leucine, L-lysine hydrochloride, L-methionine, L-phenylalanine, L-proline, L-serine, L-threonine, L-tryptophan, L-tyrosine and L-valine were used. All standards had purities ≥98% with the exception of γ-L-glutamyl–L-cysteine, which was ≥80%. All chemicals were purchased from Sigma Aldrich (St. Louis,

MO, USA). 8-Oxo-2′-deoxyguanosine-^{13}C-^{15}N$_2$ (8OhdG-^{13}C^{15}N$_2$) and phenylalanine-D$_5$ (Phe-D$_5$) were used as deuterated internal standards (IS) and were obtained from Santa Cruz Biotechnology Inc. (Texas, USA) and CDN Isotopes (Pointe-Claire, Canada), respectively, with purities ≥98%. Amicon Bioseparations Microcon-10 kDa centrifugal filter units with ultracel-10 membrane were purchased from Merck Millipore (Darmstadt, Germany).

2.2 Preparation of silver colloids for SERS measurements

Silver colloids were prepared as described by Leopold *et al.*[26] Briefly, silver nitrate (1 mM) was reduced with hydroxylamine hydrochloride (1.5 μM) at alkaline pH and room temperature. Under these conditions, the reaction is complete within a few seconds with a preparation success rate of over 90% providing silver colloids stable at room temperature. The successful synthesis of the produced silver colloidal solution was confirmed by UV-Vis spectroscopy. The absorbance maximum of the UV-Vis signal provides information on the average particle size, whereas the full width at half-maximum aids to estimate the particle dispersion. The obtained UV-Vis spectrum of the silver colloid, with an absorbance maximum of 418 nm and with a full width at half-maximum of 100 nm, is shown in the ESI, Fig. 1.† The recorded UV spectra agreed well with those reported by Leopold *et al.*, thus indicating a successful synthesis of the silver SERS colloid.[26] Transmission electron microscopic analysis of colloids providing such UV-Vis spectra revealed monodisperse particles with diameters in the range of 30–40 nm.[26] All SERS spectra were recorded using silver colloid from the same batch, as the colloid is stable at room temperature during at least three months.

2.3 Whole blood (WB) collection and storage

Umbilical cord blood samples from 5 healthy term newborn infants born by uncomplicated vaginal delivery were collected using sterile Vacutainer® tubes with K$_2$-EDTA and heparin (total: 10 WB samples). Permission was obtained by signing an informed consent. Blood samples were immediately stored at −80 °C until analysis. For UPLC-MS/MS and SERS analysis, blood samples were thawed in an ice bath. A first aliquot was processed for UPLC-MS/MS reference analysis and a second aliquot was immediately analyzed by SERS to avoid artefacts due to sample oxidation. For method optimization, blood

samples in K$_2$-EDTA tubes provided by the Austrian Red Cross were used.

2.4 Raman measurements

For protein precipitation, 150 μL of cold (4 °C) 10% v/v perchloric acid were added to 50 μL of WB. Samples were centrifuged at 12 000*g* during 5 min. 20 μL of the supernatant were mixed with 20 μL of the silver colloid, transferred to a microscopy glass slide and SERS spectra were recorded immediately. Blanks and GSH standard solutions were prepared following the same procedure as for WB samples, using 50 μL of distilled H$_2$O or standard solutions, respectively. An aqueous GSH stock solution was prepared by direct GSH standard weighing.

SERS spectra were recorded using a confocal LabRam HR800 Raman spectrometer (Horiba Jobin Yvon, Bensheim, Germany) based on an Olympus BX41 optical microscope. The microscope was equipped with a green laser emitting at 532 nm, a Nikon objective (×20, NA0.35, and WD20.5) and a 300 lines per mm grating along with a charge coupled device detector (CCD). Furthermore, neutral density filters were used to attenuate the laser beam. For spectrum acquisition, the slit width and hole were set both to 600 μm and for each spectrum two scans with an acquisition time of 10 s each were accumulated in the range between 400 and 4000 cm^{-1}. Measurement parameters were optimized in order to maximize the signal while maintaining background fluorescence at a minimum.

Partial Least Squares (PLS) regression models were developed employing the PLS Toolbox 7.8 from Eigenvector Research Inc. (Wenatchee, USA) running in Matlab 2012b from Mathworks (Natick, USA). Correlation coefficients were calculated using the corrcoef function embedded in Matlab 2012b.

2.5 UPLC-MS/MS reference measurements

Reference concentrations of GSH and other biothiols (Table 1) were obtained by UPLC-ESI(+)-MS/MS. After thawing WB samples on ice, 100 μL of the WB sample were added to 20 μL of NEM (100 mM) and homogenized on a Vortex mixer. After 1 min, the alkylation reaction was stopped and proteins were precipitated by adding 120 μL of cold (4 °C) perchloric acid at 10%. Then, the samples were centrifuged for 15 min at 12 000*g* and the supernatants were stored at −80 °C until analysis. Before analysis, samples were thawed in an ice bath and then processed by adding 100 μL of cold (4 °C) methanol to 50 μL

Table 1 Acquisition parameters of the UPLC-MS/MS method

Analyte	Cone [V]	CE [eV]	*m/z* Parent ion	*m/z* Daughter ion	RT [min]	Calibration range
Cysteine	30	20	247.1	158.1	1.130 ± 0.008	10 nM–10 μM
Homocysteine	40	15	261.3	126	1.780 ± 0.006	4 nM–2 μM
γ-Glutamylcysteine	40	25	376.1	230.1	2.320 ± 0.003	4 nM–2 μM
GSH	25	20	433.1	201	2.350 ± 0.003	6 nM–3 μM
8OhdG-^{13}C^{15}N$_2$	30	15	287	171	1.65 ± 0.01	—
Phe-D$_5$	30	20	171.5	125	1.470 ± 0.008	—

GSH: reduced glutathione, 8OhdG-^{13}C^{15}N$_2$: 8-oxo-2′-deoxyguanosine-^{13}C^{15}N$_2$, Phe-D$_5$: phenylalanine-D$_5$.

of the sample, homogenized on a vortex mixer and centrifuged at 10 000g and 4 °C for 10 min. 50 μL of the supernatant were transferred to a 96-well injection plate and mixed with 50 μL of H$_2$O (0.1% v/v HCOOH) containing 100 μM of 8OhdG-^{13}C^{15}N$_2$ and Phe-D$_5$. Samples were re-analyzed after a dilution of 1 : 50 in H$_2$O (0.1% v/v HCOOH). UPLC-MS/MS analysis was carried out using an Acquity-Xevo TQ system (Waters, Milford, MA, USA) in the positive electrospray ionization mode and under the following conditions: capillary voltage 3.2 kV, source temperature 150 °C and desolvation temperature 395 °C, respectively. Chromatographic separations were carried out on a Kinetex UPLC C8 reversed phase column (2.1 × 100 mm, 1.7 μm) and pre-column (2.1 × 2 mm) from Phenomenex (Torrance, CA, USA) using an acetonitrile (0.1% v/v HCOOH) : H$_2$O (0.1% v/v HCOOH) mobile phase gradient with a total run-time of 6 min. Flow rate, column temperature and injection volume were set at 400 μL min^{-1}, 55 °C and 3 μL, respectively. MS detection was carried out using multiple reaction monitoring (MRM) with the parameters shown in Table 1.

3.   Results and discussion

### 3.1   Raman and SERS spectra of GSH and blood samples

Raman and SERS spectra of samples and standards were obtained by using a confocal microscope employing a diode laser operating at 532 nm with an output power of 5 mW. It has to be remarked that the direct measurement of WB samples without the elimination of proteins was not possible due to the strong fluorescence background. Fig. 1 shows Raman and SERS spectra of a 1 mM GSH standard solution, a WB sample collected in a K$_2$-EDTA tube after protein removal with perchloric acid and a blank perchloric acid (7.5% v/v) solution containing the silver colloid used for SERS in the 400 and 1300 cm^{-1} range. From the results depicted in Fig. 1, a set

Table 2 Band assignments of SERS spectra between 400 and 1300 cm^{-1}

Frequency [cm^{-1}]	Vibration	Intensity	Reference
1100	$\nu_{(3)}$ band from ClO$_4^-$	w	27
925	$\nu_{(1)}$ band from ClO$_4^-$	s	27
790	Amide V band	m	24
714	$\nu_{(C-S)}$ band from $-$H$_2$C$-$S$-$ group of Cys (P$_C$ conformer)	w	24,30
642	$\nu_{(C-S)}$ band from$-$H$_2$C$-$S$-$ group of Cys (P$_H$ conformer)	s	24,30
621	$\nu_{(4)}$ band from ClO$_4^-$	w	27
456	$\nu_{(2)}$ band from ClO$_4^-$	w	27

of background signals corresponding to perchloric acid bands at 1100 (w), 925 (s), 621 (w) ad 456 (w) cm^{-1} were identified[27] (see Table 2). In addition to the blank spectrum depicted in Fig. 1, the blank spectra of H$_2$O from a K$_2$-EDTA tube and a Li-heparin tube were acquired (data not shown). The presence of EDTA and heparin in H$_2$O blanks did not cause SERS signals of significant intensities that could interfere with the GSH signal.

GSH, WB SERS spectra and regular Raman spectra of the same solutions without the Ag-NPs are also depicted in Fig. 1. Results showed clear differences in both the intensity and Raman shift of the bands between the SERS spectrum of the GSH adsorbed on Ag NPs and the spectrum in aqueous solution. Band assignments are summarized in Table 2. The intensity of distinct GSH features at 790 (m), 714 (w) and 642 (s) cm^{-1} were enhanced remarkably in SERS, enabling its detection in blood in the WB physiological concentration range. The Analytical Enhancement Factors (AEFs), calculated according to Le Ru *et al.*[28] for bands at 790 cm^{-1} (after single point baseline correction at 844 cm^{-1}) and 642 cm^{-1} (after single point baseline correction at 698 cm^{-1}), were 7.9 and 2.8,
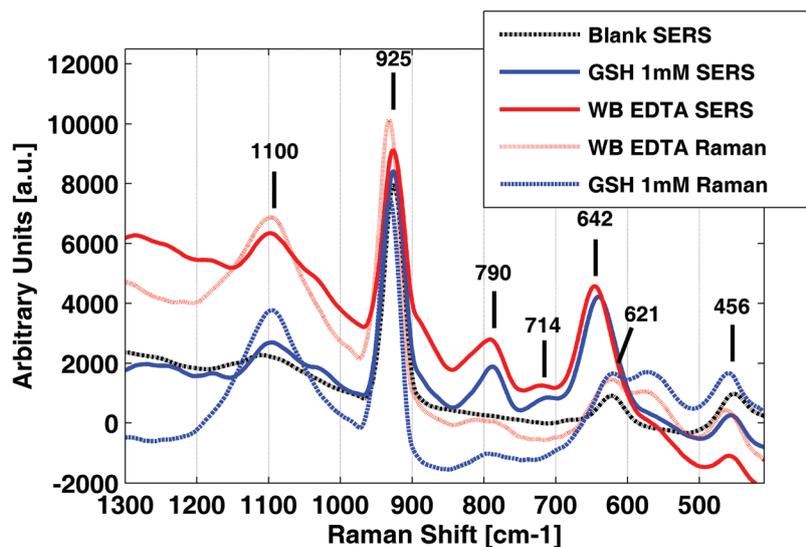
Fig. 1 SERS and Raman spectra of a glutathione (GSH) standard solution and a K$_2$-EDTA whole blood (WB) sample in comparison with a H$_2$O blank.

respectively. These AEFs values can be explained by a fixed absorption geometry, which amplifies the effect of surface selection rules.[29]

Interestingly, the recorded SERS spectra of GSH in aqueous standards and SERS spectra of WB samples were highly similar and in good agreement with previous results. Lv et al.[24] reported that the Raman spectrum of GSH adsorbed to a 3D silver nanodendrite@glass film with bands at 791, 722 and 656 cm^{-1}. Based on the Raman spectra reported for the component amino acids of GSH, the bands at 722 and 656 cm^{-1} were associated with the vibrations of the sulfur atom of the amino acid, Cys. Podstawka et al.[30] reported that a $\nu_{(C-S)}$ band from the –H$_2$C–S– group of Cys is expected in the 640–680 cm^{-1} and the 740–760 cm^{-1} regions for the P$_H$ and P$_C$ conformers of the C–S stretching vibrations, respectively. Furthermore, the band at 791 cm^{-1} was assigned to the amide V vibration due to the amide groups of glycine and glutamic acid. Lv et al.[24] conclude from their observations that GSH strongly interacts with the silver surface via the $\nu_{(C-S)}$ group and that carboxyl and amide groups are also involved in the interaction of GSH with Ag.

Signal specificity: cross-sensitivity of metabolites containing thiol functional groups. To test the specificity of the SERS signal of GSH, spectra of 21 selected L-amino acids and glycine were acquired under the described experimental conditions. Visual inspection of the SERS spectra of a GSH standard solution and the 22 considered metabolites depicted in ESI Fig. 2† indicated a highly specific GSH signal. Only for Cys a similar fingerprint was observed. Then, the correlation coefficients between the spectra of the 22 metabolites and GSH in the 400–900 cm^{-1} range were used for an unbiased quantification of signal specificity. Results summarized in Table 3 confirmed weak correlations ($R^2 < 0.75$), with the exception of Cys, that showed a considerably higher correlation coefficient of 0.90. GSH is a tripeptide containing a Cys unit that comprises a SERS active SH– functional group. Spectral correlations ≤0.4 were obtained for glycine and glutamic acid, the other two subunits of GSH, besides Cys, supporting the fact that the observed SERS signal was due to the interaction of Cys with the Ag-NP surface.

In conclusion, employing a silver colloid, and in acidic pH, molecules with an –SH functional group provide highly correlated SERS signals. The overlap of highly correlated SERS signals arising from the interactions of the SH– functional groups and the NP surface provides a measure associated with the total concentration of SH– metabolites in the sample. However, GSH concentrations in WB were reported in the mM range whereas the concentration of other biothiols is notably lower[1] and thus, the signal is largely dominated by the GSH contribution.

Effect of protein removal and pH. Proteins are very sensitive to temperature changes and the energy provided by the incident laser light causes protein coagulation. Therefore, protein removal was indispensable prior to recording SERS or Raman spectra of WB samples. Four frequent protein elimination methods were evaluated based on: (i) precipitation with cold methanol; (ii) sample acidification using perchloric acid; (iii) sample filtration using 10 kDa molecular weight filters, and (iv) a two-step clean up using filtration followed by acidification.

Protein precipitation using methanol resulted in a complete suppression of the SERS signal of GSH (results not shown). Fig. 2 shows the spectra obtained from a WB sample after protein elimination by (i) filtration, (ii) acidification with perchloric acid and (iii) after filtration followed by acidification. Protein precipitation by filtration provided characteristic SERS spectra, different to those obtained using perchloric acid, showing intense bands in the whole fingerprint region and minimal fluorescent background. However, the C–S stretching SERS bands described in section 3.1 (strongest band at 642 cm^{-1}) could not be detected. Additional band assignments in the fingerprint region can be found in previous studies.[31,32]

In order to assess whether the suppression of the SERS signal at 642 cm^{-1} was due to the loss of GSH during filtration or due to a pH change, the filtrate was acidified with perchloric acid. As shown in Fig. 2 (blue line), the SERS signal was recovered after acidification indicating that SERS activity of the C–S stretching vibrations was greatly influenced by both the pH and the protein content of the sample.

The use of molecular weight filters followed by an acidification with perchloric acid, and the direct acidification with perchloric acid for protein elimination provided comparable results. However, the latter was more straightforward and it was selected for further measurements. Nonetheless, it has to be underlined that spectral information in the 1800–1000 cm^{-1} region, obtained from filtered samples before and after acidification could be potentially useful for other determinations in WB samples.

Effect of the type of anticoagulant. Blood samples were collected employing two different anti-coagulants, K$_2$-EDTA

Table 3 Correlation coefficients (R) of SERS spectra of GSH with those of other amino acids in the range between 400 and 900 cm^{-1}

| Metabolite	R	Metabolite	R	Metabolite	R	Metabolite	R
Alanine	0.55	Glutamic	0.40	Leucine	0.52	Threonine	0.16
Arginine	0.10	Glutamine	0.60	Lysine	0.34	4-Hydroxyproline	0.45
Asparagine	0.66	Glycine	0.34	Methionine	0.33	Tryptophan	0.51
Aspartic	0.39	GSSG	0.74	Phenylalanine	0.39	Tyrosine	0.61
Cysteine	0.89	Histidine	0.27	Proline	0.53	Valine	0.33
Cystine	0.65	Isoleucine	0.11	Serine	0.23		
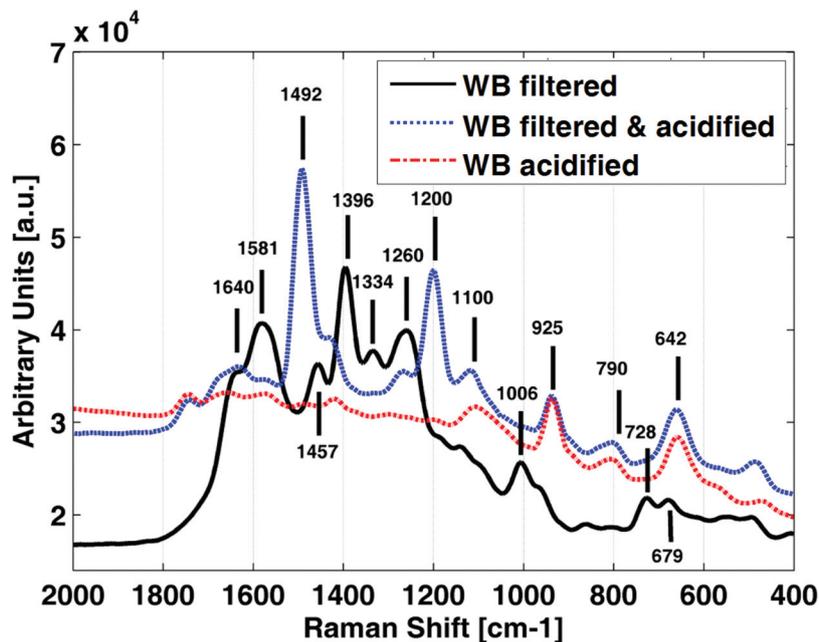
Fig. 2 SERS spectra of a K_2-EDTA whole blood (WB) sample employing different protein removal approaches; acidified with perchloric acid.

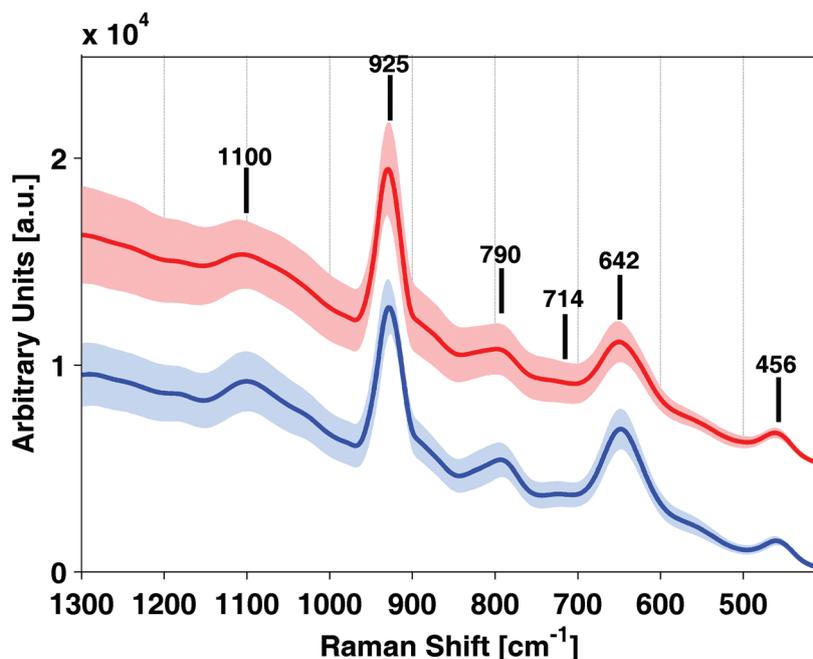**Fig. 3** Mean SERS spectra (±standard deviation) of K_2-EDTA (blue) and heparin (red) umbilical cord whole blood samples; note: heparin spectra were shifted along the y-axis; 10 replicate spectra were recorded from 5 blood samples with each coagulant.

and Li-heparin. Mean spectra (±standard deviation) of five umbilical cord blood samples collected with both anti-coagulants after acidification with perchloric acid are shown in Fig. 3. Although the band at 714 cm^{-1} was very weak, C–S Raman bands could be clearly detected in all the spectra at 648 ± 3 cm^{-1} and 650 ± 2 cm^{-1} using K_2-EDTA and Li-heparin tubes, respectively. This demonstrates that the developed

approach is capable of detecting biothiol concentrations at clinically relevant concentrations. No interfering signals due to the use of EDTA or heparin were observed in samples comparing the obtained spectral profiles to standards and blanks. However, the standard deviation for spectra obtained from heparin WB samples was higher than for EDTA WB samples, affecting the precision of the measurement.

3.2 Quantitative analysis of low molecular weight biothiols

GSH standard solutions. GSH standard solutions with concentrations ranging between 500 μM and 10 mM were prepared and five replicate SERS spectra were recorded at each of the four concentration levels after the addition of perchloric acid and the Ag SERS colloidal substrate. A PLS model was calculated by employing the 550–884 cm^{-1} spectral range. Prior to model calculation, a baseline correction (automatic weighted least squares) was carried out followed by Savitzky–Golay smoothing and mean centering. Fig. 4 shows the predicted values by leave-one-out cross validation using nine latent variables obtaining a RMSECV of 1740 μM and an R^2 of 0.99. This result demonstrates that there is a linear correlation between GSH concentration and SERS signal in analytical standard solutions.

Quantitative analysis of low molecular weight biothiols in WB. Homocysteine, γ-glutamylcysteine, Cys and GSH concentrations were determined in blood samples collected in Li-heparin and K$_2$-EDTA tubes by a reference UPLC-MS/MS procedure. Results provided by UPLC-MS/MS in Table 4 showed that, as expected, the concentration of GSH represents >90% of the considered thiols in WB samples. GSH concentrations in WB of 865.5 ± 266.5 μM, 861.7 ± 235.3 μM ($N = 67$)[33] and 900 ± 140 μM ($N = 59$)[8] have been previously reported for

healthy adults. These values are comparable to the GSH concentrations in umbilical cord WB samples of neonates found in previous studies (1000 ± 160 μM ($N = 26$)[4] and 1000 ± 170 μM ($N = 22$)[34]). Previously reported GSH concentration ranges were statistically comparable (t-test, $p > 0.05$) to the values summarized in Table 4.

In addition, a blood sample collected with each anti-coagulant was kept at 4 °C during 24 h and the analysis was repeated to monitor the changes due to sample oxidation. Thiol concentrations were significantly lower with RSH concentrations of 13 and 239 μM for EDTA and heparin WB, respectively, as determined by UPLC-MS/MS. However, GSH remained the most abundant biothiol with >78% of RSH.

Using the total concentration of the determined biothiols (RSH) [μM] as a predictive variable, the performance of a quantitative method based on SERS measurements of WB samples was evaluated. A PLS model was calculated employing the same spectral preprocessing and range as used for standard solutions and EDTA blood samples with concentrations ranging between 13 and 2200 μM. Fig. 5a shows the predicted values by leave-one-out cross validation using three latent variables obtaining a RMSECV of 291 μM and an R^2 of 0.92. The model was applied to EDTA and heparin blood samples with total RSH concentrations ranging between 239 and 1959 μM (see Fig. 5a) achieving an RMSEP of 381 μM. It has to be high-
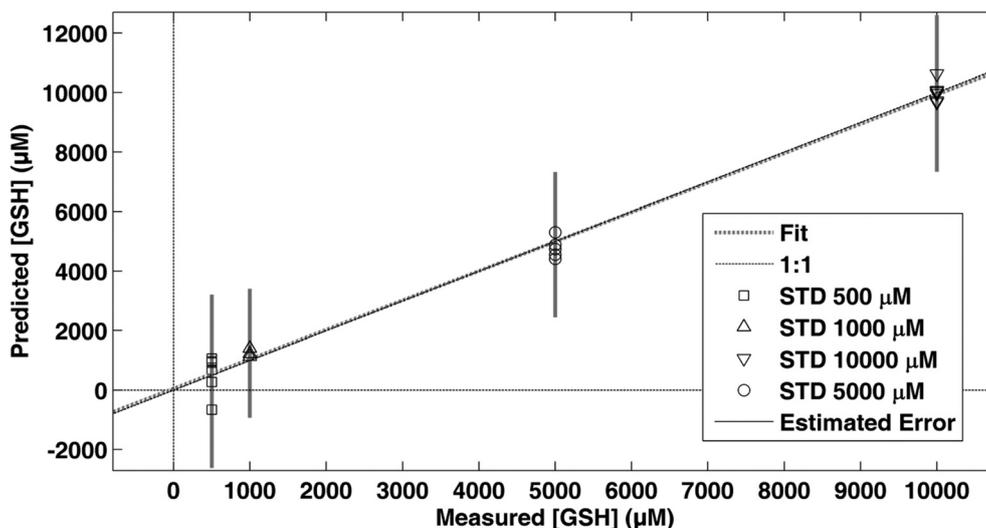

Fig. 4 Quantification of GSH standard solution employing the SERS method and a multivariate PLS model using the spectral region between 550 and 884 cm^{-1}.

Table 4 Concentration of glutathione (GSH) and total concentration of biothiols (RSH) determined in whole blood samples by the UPLC-MS/MS reference method. Note: all concentrations are given in μM

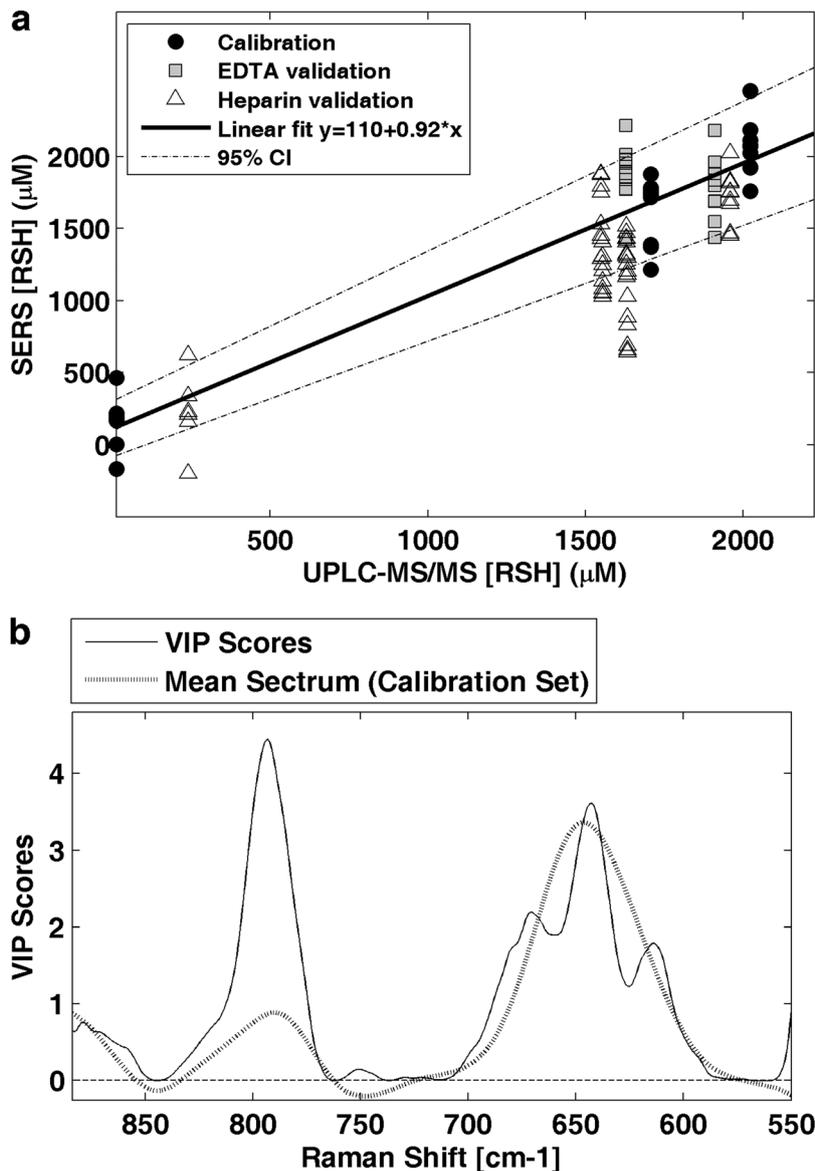| Parameter	Homocysteine	γ-Glutamylcysteine	Cysteine	GSH	RSH	% GSH
Mean ± s	2.8 ± 1.2	18 ± 12	90 ± 40	1300 ± 600	1400 ± 700	91 ± 5
Median	3.2	13	105	1490	1630	91
Range	0.3–3.9	0.05–31	3–141	10–1949	13–2022	78–96

Fig. 5 Quantification of total concentration of determined biothiols (RSH) in whole blood (WB) samples employing SERS. RSH concentrations determined by UPLC-MS/MS vs. SERS (a) and VIP scores of the PLS model (b). Note: the mean spectrum of the calibration set was scaled and included for an easier interpretation in (b).

lighted, that the spectral features of biothiols were not influenced by the type of anticoagulant, enabling the use of EDTA and heparin blood samples. Fig. 5b shows the Variable Importance in Projection (VIP) scores of the calculated model in comparison with the mean spectrum of the calibration set. VIP scores estimate the importance of each variable in the projection used in a PLS model. In a given model, a variable with a VIP score close to or greater than one is typically considered important.[35] Here, it can be observed that the most intense VIP scores match the thiol SERS bands at 790 and 642 cm^{-1}.

These preliminary results demonstrate the feasibility of the direct quantification of low molecular weight biothiols in WB samples at clinically relevant concentrations by SERS.

Although for clinical applications the precision of the measurement has to be improved, a statistically significant correlation between the concentration of biothiols measured by UPLC-MS/MS and SERS was obtained.

4 Conclusions

This new approach involves the use of a silver colloid for SERS detection of biothiols in WB samples. Biothiols interact with the silver surface via the $v_{(C–S)}$ group and carboxyl and amide groups are also involved. The recorded spectral features of GSH, which is the most abundant biothiol, could be assigned

to the $\nu_{(C-S)}$ vibration from thiols (714 and 642 cm^{-1}) and to the amide V band (at 790 cm^{-1}). Signal specificity was tested by recording the SERS spectra of 21 amino acids with similar structures as well as glycine; SERS bands could only be detected in the case of molecules presenting –SH functional groups (*e.g.* cysteine).

In whole blood samples, protein removal and acidic pH were necessary for obtaining SERS signals from molecules with a –SH functional group. The developed approach uses small blood sample volumes of only 50 µL, which is important for applications in the field of neonatology. A correlation of SERS signal and biothiol concentration in umbilical cord WB samples could be demonstrated. Further studies are necessary for determining the analytical figures of merit including limits of detection and quantification, linear range, accuracy and precision.

This approach meets the requirements for its potential application in clinical studies, as sample treatment, analysis time and blood volumes were minimized. Yet, at the current stage, some practical limitations are encountered which have to be tackled in the future to clear the way for this technique in the clinic. First, measurement precision and repeatability will have to be improved. Further research on the effect of the physicochemical properties of the silver colloids, and on auto-mated sampling and data acquisition procedures will be carried out to improve the measurement process and the repeatability and sensitivity of the measurement (*i.e.* strong and stable enhancement factors). Furthermore it will be of utmost importance to enable the simultaneous determination of oxidized biothiols in order to obtain an indication of the redox status typically employed in clinics. Here, paper-based plasmonic platforms could potentially play an important role.[36–38] These emerging devices would be suitable for a point-of-care testing system combined with adequate experi-mental acquisition parameters. Moreover, these platforms allow the incorporation of different sample treatments, *e.g.* the surface chemical gradient created by differential polyelectro-lyte coatings of paper.[39]

Acknowledgements

References

1 M. Isokawa, T. Kanamori, T. Funatsu and M. Tsunoda, *J. Chromatogr., B: Biomed. Appl.*, 2014, **964**, 103–115.
2 T. J. van 't Erve, B. A. Wagner, K. K. Ryckman, T. J. Raife and G. R. Buettner, *Free Radicals Biol. Med.*, 2013, **65**, 742–749.
3 D. Giustarini, P. Fanti, E. Matteucci and R. Rossi, *J. Chromatogr., B: Biomed. Appl.*, 2014, **964**, 191–194.
4 M. Vento, M. Asensi, J. Sastre, F. García-Sala, F. V. Pallardó and J. Viña, *Pediatrics*, 2001, **107**, 642–647.
5 J. Viña, M. Vento, F. García-Sala, I. R. Puertes, E. Gascó, J. Sastre, M. Asensi and F. V. Pallardó, *Am. J. Clin. Nutr.*, 1995, **61**, 1067–1069.
6 M. Asensi, J. Sastre, F. V. Pallardo, J. M. Estrela and J. Viña, *Methods Enzymol.*, 1994, **234**, 367–371.
7 R. L. G. Norris, M. Paul, R. George, A. Moore, R. Pinkerton, A. Haywood and B. Charles, *J. Chromatogr., B: Biomed. Appl.*, 2012, **898**, 136–140.
8 T. Moore, A. Le, A.-K. Niemi, T. Kwan, K. Cusmano-Ozog, G. M. Enns and T. M. Cowan, *J. Chromatogr., B: Biomed. Appl.*, 2013, **929**, 51–55.
9 K. Kowalska, M. Zalewska and H. Milnerowicz, *J. Chroma-togr. Sci.*, 2015, **53**(2), 353–359.
10 I. Rahman, A. Kode and S. K. Biswas, *Nat. Protoc.*, 2007, **1**, 3159–3165.
11 P. Monostori, G. Wittmann, E. Karg and S. Túri, *J. Chromatogr., B: Biomed. Appl.*, 2009, **877**, 3331–3346.
12 A. L. Mitchell, K. B. Gajjar, G. Theophilou, F. L. Martin and P. L. Martin-Hirsch, *J. Biophotonics*, 2014, **7**, 153–165.
13 D. Perez-Guaita, S. Garrigues and M. de la Guardia, *TrAC Trends Anal. Chem.*, 2014, **62**, 93–105.
14 S. Pahlow, A. März, B. Seise, K. Hartmann, I. Freitag, E. Kämmer, R. Böhme, V. Deckert, K. Weber, D. Cialla and J. Popp, *Eng. Life Sci.*, 2012, **12**, 131–143.
15 H. Abramczyk and B. Brozek-Pluska, *Chem. Rev.*, 2013, **113**, 5766–5781.
16 A. Bonifacio, S. Cervo and V. Sergo, *Anal. Bioanal. Chem.*, 2015, **407**, 8265–8277.
17 M.-E. Gosselin, C. J. Kapustij, U. D. Venkateswaran, V. R. Leverenz and F. J. Giblin, *Exp. Eye Res.*, 2007, **84**, 493–499.
18 E. Zachariah, A. Bankapur, C. Santhosh, M. Valiathan and D. Mathur, *J. Photochem. Photobiol., B*, 2010, **100**, 113–116.
19 G. G. Huang, M. K. Hossain, X. X. Han and Y. Ozaki, *Analyst*, 2009, **134**, 2468–2474.
20 A. Saha and N. R. Jana, *Anal. Chem.*, 2013, **85**, 9221–9228.
21 L. Ouyang, L. Zhu, J. Jiang and H. Tang, *Anal. Chim. Acta*, 2014, **816**, 41–49.
22 G. G. Huang, X. X. Han, M. K. Hossain and Y. Ozaki, *Anal. Chem.*, 2009, **81**, 5881–5888.

23 P. Singh, N. T. B. Thuy, Y. Aoki, D. Mott and S. Maenosono, *J. Appl. Phys.*, 2011, **109**, 094301.

24 M. Lv, H. Gu, X. Yuan, J. Gao and T. Cai, *J. Mol. Struct.*, 2012, **1029**, 75–80.

25 S. Ma and Q. Huang, *RSC Adv.*, 2015, **5**, 57847–57852.

26 N. Leopold and B. Lendl, *J. Phys. Chem. B*, 2003, **107**, 5723–5727.

27 C. I. Ratcliffe and D. E. Irish, *Can. J. Chem.*, 1984, **62**, 1134–1144.

28 E. C. Le Ru, E. Blackie, M. Meyer and P. G. Etchegoin, *J. Phys. Chem. C*, 2007, **111**, 13794–13803.

29 M. Moskovits and J. S. Suh, *J. Phys. Chem.*, 1984, **88**, 5526–5530.

30 E. Podstawka, Y. Ozaki and L. M. Proniewicz, *Appl. Spectrosc.*, 2004, **58**, 570–580.

31 B. R. Wood, P. Caspers, G. J. Puppels, S. Pandiancherri and D. McNaughton, *Anal. Bioanal. Chem.*, 2006, **387**, 1691–1703.

32 E. Staniszewska-Slezak, K. Malek and M. Baranska, *Spectrochim. Acta, Part A*, 2015, **147**, 245–256.

33 I. Squellerio, D. Caruso, B. Porro, F. Veglia, E. Tremoli and V. Cavalca, *J. Pharm. Biomed. Anal.*, 2012, **71**, 111–118.

34 M. Vento, M. Asensi, J. Sastre, A. Lloret, F. García-Sala and J. Viña, *J. Pediatr.*, 2003, **142**, 240–246.

35 I.-G. Chong and C.-H. Jun, *Chemom. Intell. Lab. Syst.*, 2005, **78**, 103–112.

36 Q. Liu, J. Wang, B. Wang, Z. Li, H. Huang, C. Li, X. Yu and P. K. Chu, *Biosens. Bioelectron.*, 2014, **54**, 128–134.

37 B. Nie, Q. Zhou, J. He and F. Yang, *J. Raman Spectrosc.*, 2015, **46**, 211–216.

38 D. M. Cate, J. A. Adkins, J. Mettakoonpitak and C. S. Henry, *Anal. Chem.*, 2015, **87**, 19–41.

39 A. Abbas, A. Brimer, J. M. Slocik, L. Tian, R. R. Naik and S. Singamaneni, *Anal. Chem.*, 2013, **85**, 3977–3983.